

Extending Galton's Binomial Quincunx to the Trinomial Septcunx

Jenny Harlow, Bry Ashman and Raazesh Sainudiin

Laboratory for Mathematical Statistical Experiments

Department of Mathematics and Statistics

University of Canterbury

Private Bag 4800

Christchurch, New Zealand



UCDMS 2009/6. Some rights reserved.

This work is licensed under the Creative Commons Attribution-NonCommercial-Share Alike 3.0 New Zealand Licence. To view a copy of this license, visit

<http://creativecommons.org/licenses/by-nc-sa/3.0/nz/>.

Abstract

This paper discusses the development of graphical user interfaces (GUIs) to illustrate sampling from a trinomial distribution by the natural extension of Galton's Quincunx to three dimensions.

Keywords: Multinomial distribution, GUI, vector addition, Galton's binomial Quincunx and the trinomial Septcunx.

1. Introduction and Motivation

The visual or graphical display of data as part of statistical analysis is commonly dated to the late 18th century when Priestly and Playfair used graphics to illustrate their works. Since Tukey's influential *Exploratory Data Analysis* (Tukey, 1977), visual displays have become increasingly important. Developments in computing power and graphics hardware and software have been exploited to be able to handle and visualise datasets of a size and complexity that would probably stun Tukey, let alone Playfair (Card, Mackinlay & Shneiderman, 1999). The principles for good visual displays, such as those set out in Tufte's classic *The Visual Display of Quantitative Information* (Tufte, 1983) and the deployment of computing power for the graphical display of statistical data have been focused on rapid data analysis and interpretation.

For students, graphics may need to fulfil a different role. When data are displayed, often it is the illustration of concepts through data rather than analysis of the data itself that is important; the emphasis changes from information density to information clarity. Computer packages offer powerful graphics capabilities for data analysis but learning to use the package

may distract from the central point of understanding the concepts (Nolan & Temple, 2003). Sedig & Liang (2008) use the term visual cognitive tools (VCTs) for the “external mental aids that maintain and display visual representations of information”, where ‘information’ here means “structures, objects, concepts, ideas and problems” (Sedig & Liang, 2008, p. 147), not just the data in an investigation. Graphical displays which are ideal for data analysis have to be adapted for students in order to become an effective VCT to illustrate the actual processes undertaken by the statistician or elucidate an underlying principle.

This paper presents a project to create a VCT for graphically illustrating the binomial coefficient and, by extension, the trinomial coefficient. We start by revisiting Sir Francis Galton’s Quincunx. We formalise a probability model of the Quincunx as a binomial random vector via sums of two-dimensional Bernoulli random vectors. We show how the Quincunx can be used to demonstrate the binomial coefficient graphically with the paths leading to an outcome. We extend the Quincunx in a natural manner to its three-dimensional version called the Septcunx. The probability model for the Septcunx is the trinomial random vector obtained by a sum of IID trivariate random vectors. Again, the trinomial coefficient can be demonstrated graphically.

The model of the Quincunx could be further extended to demonstrate the Poisson approximation to the binomial, asymptotic consistency of the maximum likelihood estimator and even Bayesian inference. The trinomial model could be extended to demonstrate the equivalence of sum-conditional Poisson to the trinomial, the law of large numbers and the central limit theorem for random vectors, and asymptotic consistency of the MLE of vector parameters.

2. Sir Francis Galton’s Quincunx

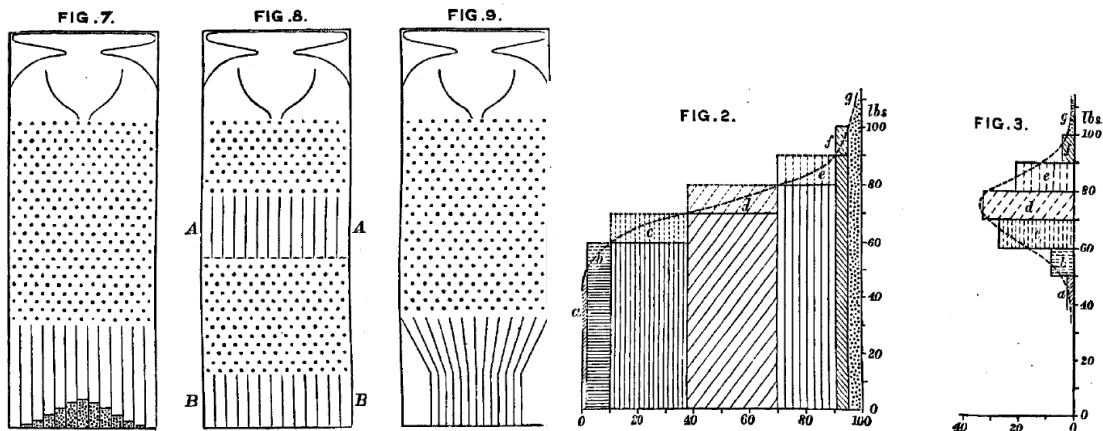
We first quote the following words from Sir Francis Galton’s historic work, *Natural Inheritance*, pp. 62-65, Macmillan, 1889. Here you will find the kernels behind the construction of the Binomial(θ) RV as the sum of IID Bernoulli(θ) RVs, Bernoulli’s Weak Law of Large Numbers and the Central Limit Theorem.

“The Charms of Statistics.—It is difficult to understand why statisticians commonly limit their inquiries to Averages, and do not revel in more comprehensive views. Their souls seem as dull to the charm of variety as that of the native of one of our flat English counties, whose retrospect of Switzerland was that, if its mountains could be thrown into its lakes, two nuances would be got rid of at once. An Average is but a solitary fact, whereas if a single other fact be added to it, an entire Normal Scheme, which nearly corresponds to the observed one, starts potentially into existence.

Some people hate the very name of statistics, but I find them full of beauty and interest. Whenever they are not brutalised, but delicately handled by the higher methods, and are warily interpreted, their power of dealing with complicated phenomenon is extraordinary. They are the only tools by which an opening can be cut through the formidable thicket of difficulties that bars the path of those who pursue the Science of man.

Mechanical Illustration of the Cause of the Curve of Frequency.—The Curve of Frequency, and

Figure 1: Figures from Sir Francis Galton, F.R.S., *Natural Inheritance*, Macmillan, 1889.



(a) FIG. 7, FIG. 8, and FIG. 9 (p. 63)

(b) FIG. 2 and FIG. 3 (p. 38)

that of *Distribution*, are convertible : therefore if the genesis of either of them can be made clear, that of the other also becomes intelligible. I shall now illustrate the origin of the *Curve of Frequency*, by means of an apparatus shown in Fig. 7, that mimics in a very pretty way the conditions on which *Deviation* depends. It is a frame glazed in front, leaving a depth of about a quarter of an inch behind the glass. Strips are placed in the upper part to act as a funnel. Below the outlet of the funnel stand a succession of rows of pins stuck squarely into the backboard, and below these again are a series of vertical compartments. A charge of small shot is inclosed. When the frame is held topsy-turvy, all the shot runs to the upper end; then, when it is turned back into its working position, the desired action commences. Lateral strips, shown in the diagram, have the effect of directing all the shot that had collected at the upper end of the frame to run into the wide mouth of the funnel. The shot passes through the funnel and issuing from its narrow end, scampers deviously down through the pins in a curious and interesting way; each of them darting a step to the right or left, as the case may be, every time it strikes a pin. The pins are disposed in a quincunx fashion, so that every descending shot strikes against a pin in each successive row. The cascade issuing from the funnel broadens as it descends, and, at length, every shot finds itself caught in a compartment immediately after freeing itself from the last row of pins. The outline of the columns of shot that accumulate in the successive compartments approximates to the *Curve of Frequency* (Fig. 3, p. 38), and is closely of the same shape however often the experiment is repeated. The outline of the columns would become more nearly identical with the *Normal Curve of Frequency*, if the rows of pins were much more numerous, the shot smaller, and the compartments narrower; also if a larger quantity of shot was used.

The principle on which the action of the apparatus depends is, that a number of small and independent accidents befall each shot in its career. In rare cases, a long run of luck continues to favour the course of a particular shot towards either outside place, but in the large majority of instances the number of accidents that cause *Deviation* to the right, balance in a greater or less degree those that cause *Deviation* to the left. Therefore most of the shot finds its way into the compartments that are situated near to a perpendicular line drawn from the outlet of

the funnel, and the Frequency with which shots stray to different distances to the right or left of that line diminishes in a much faster ratio than those distances increase. This illustrates and explains the reason why mediocrity is so common.”

We will mathematically present these concepts in the sequel as a way of giving precise meanings to Galton’s observations with his Quincunx and its three-dimensional extension to our Septcunx. Then we show how our GUI interactively builds the binomial and trinomial distributions from these historic devices. In the process we will animate how the sum of bivariate Bernoulli and trivariate de Moivre random vectors yield the binomial and trinomial random vectors, respectively.

We can relate a discrete probability model to the Quincunx. First, we need to introduce simple random vectors ($R\vec{V}$), i.e. ordered pairs, ordered triples, or more generally ordered m -tuples of random variables (X_1, X_2, \dots, X_m) . We focus on elementary definitions needed to define bivariate $R\vec{V}$ obtained from a pair of random variables. Here is a simple example of a discrete bivariate $R\vec{V}$ that illustrates the notions of joint and marginal probabilities.

Example 1. *Let X_1 and X_2 be a pair of IID Bernoulli(1/2) RVs each taking values in the set $\{0, 1\}$ with the following joint probabilities:*

	$X_2 = 0$	$X_2 = 1$	
$X_1 = 0$	1/4	1/4	1/2
$X_1 = 1$	1/4	1/4	1/2
	1/2	1/2	1

From the above Table we can read for instance that the joint probability $\mathbf{P}((X_1, X_2) = (0, 0)) = 1/4$ and that the marginal probability $\mathbf{P}(X_1 = 0) = 1/2$.

Let us consider the natural two-dimensional analogue of the Bernoulli(θ) random vector in the real plane $\mathbb{R}^2 := (-\infty, \infty)^2 := (-\infty, \infty) \times (-\infty, \infty)$. A natural possibility is to use the **ortho-normal basis vectors** in \mathbb{R}^2 :

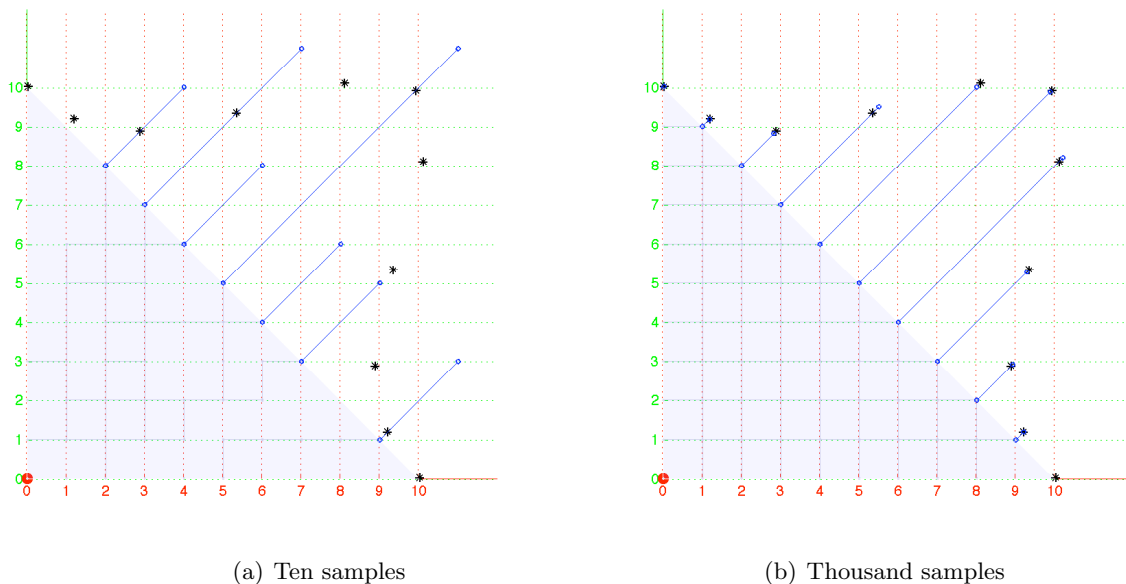
$$\boxed{e_1 := (1, 0), \quad e_2 := (0, 1)}.$$

This representation utilises the laws of vector addition and subtraction, which are performed component-wise, i.e. $(x_1, x_2) \pm (y_1, y_2) = (x_1 \pm y_1, x_2 \pm y_2)$. Let $\mathbf{1}_A(x)$ be the indicator function of set A , i.e. $\mathbf{1}_A(x) = 1$ if $x \in A$ and $\mathbf{1}_A(x) = 0$ if $x \notin A$.

Model 1 (Bernoulli(θ) $R\vec{V}$). *Given a parameter $\theta \in [0, 1]$, we say that $X := (X_1, X_2)$ is a Bernoulli(θ) random vector ($R\vec{V}$) if it has only two possible outcomes in the set $\{e_1, e_2\} \subset \mathbb{R}^2$, i.e. $x := (x_1, x_2) \in \{(1, 0), (0, 1)\}$. The PMF of the $R\vec{V}$ $X := (X_1, X_2)$ with realisation $x := (x_1, x_2)$ is:*

$$f(x; \theta) := \mathbf{P}(X = x) = \theta \mathbf{1}_{\{e_1\}}(x) + (1 - \theta) \mathbf{1}_{\{e_2\}}(x) = \begin{cases} \theta & \text{if } x = e_1 := (1, 0) \\ 1 - \theta & \text{if } x = e_2 := (0, 1) \\ 0 & \text{otherwise} \end{cases}$$

Figure 2: Quincunx on the Cartesian plane. *The outline of the columns of shot that accumulate in the successive compartments approximates to the Curve of Frequency (Galton 1889).*



We can write the Binomial(n, θ) RV Y as a Binomial(n, θ) $R\vec{V}(Y, n - Y)$. In the coin-tossing context this can be thought of keeping track of the number of Heads and Tails out of an IID sequence of n tosses of a coin with probability θ of observing Heads. In the Quincunx context, as depicted in Figure 2, this amounts to keeping track of the number of right and left turns made by the ball as it drops through n levels of pegs where the probability of a right turn at each peg is independently and identically θ .

Model 2 (Binomial(n, θ) $R\vec{V}$). *The Binomial(n, θ) $R\vec{V}(Y, n - Y)$ is the sum of n IID Bernoulli(θ) $R\vec{V}$ s $X_1 := (X_{1,1}, X_{1,2}), X_2 := (X_{2,1}, X_{2,2}), \dots, X_n := (X_{n,1}, X_{n,2})$:*

$$(Y, n - Y) = X_1 + X_2 + \dots + X_n = (X_{1,1}, X_{1,2}) + (X_{2,1}, X_{2,2}) + \dots + (X_{n,1}, X_{n,2})$$

Binomial(n, θ) $R\vec{V}(Y, n - Y)$ has the PMF given by:

$$f(y; n, \theta) := \mathbf{P}(Y = y; n, \theta) = \binom{n}{y} \theta^y (1 - \theta)^{n-y} ,$$

where, the binomial coefficient that gives the number of distinct paths from the origin $(0, 0)$ to the sample point $(y, n - y)$ in the Quincunx of Figure 2 is:

$$\binom{n}{y} := \frac{n!}{y!(n - y)!} .$$

In our depiction of Galton's quincunx in Cartesian coordinates, as done in Figure 2, the top of the original mechanical quincunx, the release point of each ball or shot, is mapped

by a 90 degree rotation to the origin $(0, 0)$ to conform to the standard ortho-normal two-dimensional Euclidean coordinate system. Figure 2 may be interpreted as simulations of a Binomial($n = 10, \theta = 0.5$) $\vec{R}\vec{V}$ as the ordered pair resulting from the culmination of sample trajectories formed by the accumulating sum of $n = 10$ IID Bernoulli($\theta = 0.5$) random vectors over $\{(1, 0), (0, 1)\}$ with probabilities $\{\theta, 1 - \theta\}$, respectively. The blue stem plots and black asterisks perpendicular to and above the diagonal line, i.e. the line connecting $(0, 10)$ and $(10, 0)$, are the density histogram of the samples and the PDF of our Binomial($n = 10, \theta = 0.5$) $\vec{R}\vec{V}$, respectively.

Note that with only 10 sample trajectories of 10 independent balls in Figure 2(a), the density histogram of the samples depicted by blue stem plots are different from the PDF of the Binomial($n = 10, \theta = 0.5$) $\vec{R}\vec{V}$ depicted by black asterisks. However, in Figure 2(b), with 1,000 sample trajectories, we can see that the stem plots are reaching the asterisks to illustrate Galton's observation: *The outline of the columns of shot that accumulate in the successive compartments approximates to the Curve of Frequency. The Curve of Frequency* referred to by Galton here is the PDF of the Binomial($n = 10, \theta = 0.5$) $\vec{R}\vec{V}$ denoted by black asterisks and his reference to *The outline of the columns of shot that accumulate in the successive compartments* is merely the outline formed by the top of our blue stem plots of the density histograms. This phenomenon is formally known as convergence in distribution.

We can extend the Binomial(n, θ) RV or $\vec{R}\vec{V}$ to the Multinomial($n, \theta_1, \theta_2, \dots, \theta_k$) random vector, its multivariate extension. The multinomial distribution is a discrete probability distribution which can be thought of as the outcome from n independent trials where each trial results in exactly one of some fixed finite number k of possible outcomes and the probability $f(i)$ of outcome $i \in \{1, 2, \dots, k\}$ in any one trial is θ_i , such that $\sum_{i=1}^k \theta_i = 1$ and $f(i) = 0$ for $i \notin \{1, 2, \dots, k\}$. A multinomial random variable parameterised by (n, θ) is a random vector $X = (X_1, X_2, \dots, X_k)$ where each X_i is the number of times that outcome $i \in \{1, 2, \dots, k\}$ is observed in the n trials and $\theta = (\theta_1, \theta_2, \dots, \theta_k)$. The binomial is the $k = 2$ case of the multinomial.

In the same way as the binomial distribution can be thought of as the sum of n IID Bernoulli(θ) $\vec{R}\vec{V}$ s, we develop the multinomial random vector as the sum of n IID de Moivre($\theta_1, \theta_2, \dots, \theta_k$) $\vec{R}\vec{V}$ s.

Model 3 (de Moivre($\theta_1, \theta_2, \dots, \theta_k$) $\vec{R}\vec{V}$). *The PMF of the de Moivre($\theta_1, \theta_2, \dots, \theta_k$) random vector $X := (X_1, X_2, \dots, X_k)$ taking value $x := (x_1, x_2, \dots, x_k) \in \{e_1, e_2, \dots, e_k\}$, where the e_i 's are ortho-normal basis vectors in \mathbb{R}^k is:*

$$f(x; \theta_1, \theta_2, \dots, \theta_k) := \mathbf{P}(X = x) = \sum_{i=1}^k \theta_i \mathbf{1}_{\{e_i\}}(x) := \begin{cases} \theta_1 & \text{if } x = e_1 := (1, 0, \dots, 0) \in \mathbb{R}^k \\ \theta_2 & \text{if } x = e_2 := (0, 1, \dots, 0) \in \mathbb{R}^k \\ \vdots & \\ \theta_k & \text{if } x = e_k := (0, 0, \dots, 1) \in \mathbb{R}^k \\ 0 & \text{otherwise} \end{cases}$$

Of course, $\sum_{i=1}^k \theta_i = 1$.

When we add n IID de Moivre($\theta_1, \theta_2, \dots, \theta_k$) $\vec{R}\vec{V}$ s together, we get the Multinomial($n, \theta_1, \theta_2, \dots, \theta_k$) random vector, which is defined below.

Model 4 (Multinomial($n, \theta_1, \theta_2, \dots, \theta_k$) $R\vec{V}$). We say that a $R\vec{V} Y := (Y_1, Y_2, \dots, Y_k)$ obtained from the sum of n IID de Moivre($\theta_1, \theta_2, \dots, \theta_k$) $R\vec{V}$ s with realisations

$$y := (y_1, y_2, \dots, y_k) \in \mathbb{Y} := \{(y_1, y_2, \dots, y_k) \in \mathbb{Z}_+^k : \sum_{i=1}^k y_i = n\}$$

has the PMF given by:

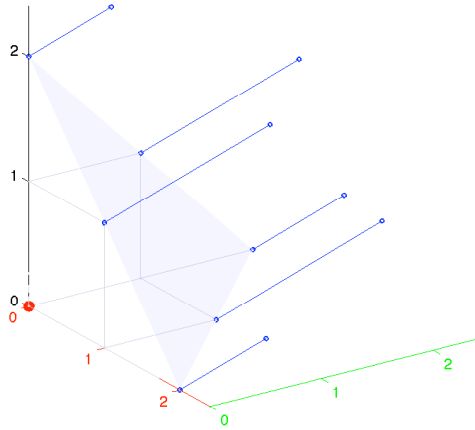
$$f(y; n, \theta) := f(y; n, \theta_1, \theta_2, \dots, \theta_k) := \mathbf{P}(Y = y; n, \theta_1, \theta_2, \dots, \theta_k) = \binom{n}{y_1, y_2, \dots, y_k} \prod_{i=1}^k \theta_i^{y_i},$$

where the multinomial coefficient:

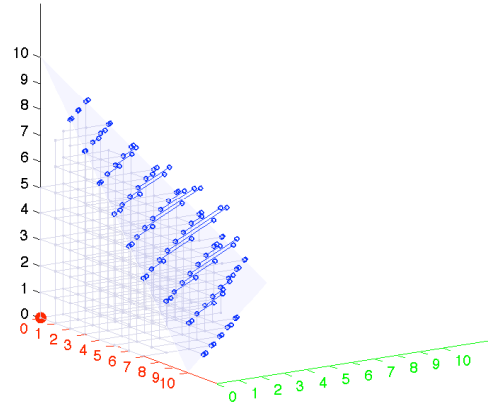
$$\binom{n}{y_1, y_2, \dots, y_k} := \frac{n!}{y_1! y_2! \dots y_k!}.$$

Note that the marginal PMF of Y_j is Binomial(n, θ_j) for any $j = 1, 2, \dots, k$.

Figure 3: Septcunx on the Cartesian co-ordinates. Simulations of Multinomial($n = 2, \theta_1 = 1/3, \theta_2 = 1/3, \theta_3 = 1/3$) $R\vec{V}$ as the sum of n IID de Moivre($\theta_1 = 1/3, \theta_2 = 1/3, \theta_3 = 1/3$) $R\vec{V}$ s over $\{(1, 0, 0), (0, 1, 0), (0, 0, 1)\}$ with probabilities $\{\theta_1, \theta_2, \theta_3\}$, respectively. The blue lines perpendicular to the sample space of the Multinomial($3, \theta_1, \theta_2, \theta_3$) $R\vec{V}$, i.e. the plane in \mathbb{R}^3 connecting $(n, 0, 0)$, $(0, n, 0)$ and $(0, 0, n)$, are the density histogram of the samples.



(a) Thousand Samples with $n = 2$



(b) Thousand Samples with $n = 10$

We can visualise the Multinomial($n, \theta_1, \theta_2, \theta_3$) process as a sum of n IID de Moivre($\theta_1, \theta_2, \theta_3$) $R\vec{V}$ s via a three dimensional extension of the Quincunx called the ‘‘Septcunx’’ and relate the number of paths that lead to a given trivariate sum (y_1, y_2, y_3) with $\sum_{i=1}^3 y_i = n$ as

the multinomial coefficient $\frac{n!}{y_1!y_2!y_3!}$. In the Septcunx, balls choose from one of three paths along e_1 , e_2 and e_3 with probabilities θ_1 , θ_2 and θ_3 , respectively, in an IID manner at each of the n levels, before they collect at buckets placed at the integral points in the 3-simplex, $\mathbb{Y} = \{(y_1, y_2, y_3) \in \mathbb{Z}_+^3 : \sum_{i=1}^3 y_i = n\}$. Once again, we can visualise that the sum of n IID de Moivre($\theta_1, \theta_2, \theta_3$) R \vec{V} s constitute the Multinomial($n, \theta_1, \theta_2, \theta_3$) R \vec{V} as depicted in Figure 3. For simplicity, in this project the multinomials used have $\theta_i = \frac{1}{k}$, i.e., each of the $i \in \{1, 2, \dots, k\}$ outcomes of a single trial is equally likely.

3. Visual Cognitive Tool for Quincunx and Septcunx

The VCT GUI requires a way to represent the the binomial and trinomial distribution visually. In this project, a directional travel analogy is used. The sequence of trials is represented as a journey in which the outcome of any of the n trials is interpreted as the direction taken at that point (out of k possible directions) and the final outcome can be interpreted in terms of an end point of the journey in relation to the starting point. A multinomial random vector $X = (X_1, X_2, \dots, X_k)$ is the summative effect of n separate independent and identically distributed directional movements.

For this project, the direction analogy is interpreted as travel in orthogonal directions. A multinomial random vector $X = (X_1, X_2, \dots, X_k)$ is considered as the sum of n independent and identically distributed trials in which the result of any one trial is e_i , the i^{th} orthonormal basis vector (the k -dimensional vector where all elements except the i^{th} are 0 and the i^{th} element is 1).

In keeping with the Quincunx approach, the GUI depicts a sample, when in motion (i.e., accumulating its trials, or the equivalent of dropping from peg to peg for the Quincunx), as a ball. The GUI represents the ‘path’ taken by a particular sample or ball. For any trial (or stage of the journey) m ($1 \leq m \leq n$), a sample x can be thought of as being at the point represented by $\sum_{j=1}^m e_j$ where e_j is the ortho-normal basis vector which is the outcome of the j^{th} trial (i.e., either (1,0) or (0,1)). This point can be plotted on the Cartesian (x, y) coordinates for each $m = 1, 2, \dots, n$ and thus the ‘path’ of the sample plotted. This demonstrates that different paths can lead to the same outcome in the sample space and provides a visual interpretation of the binomial coefficient $\binom{n}{x}$ as the number of distinct paths that can lead to the same destination point at level n .

The Binomial case when $k = 2$ can be visually represented on the Cartesian (x, y) coordinates. Using this analogy, each trial can result in travel either in the direction (1,0) or the direction (0,1). The model used in the project assumes that $\theta = (\frac{1}{2}, \frac{1}{2})$, i.e., in any trial, travel in the x , or y directions is equally likely. Thus any outcome in the sample space of all possible outcomes can be represented visually as points in (x, y) Cartesian coordinates.

The same approach can be taken when $k = 3$, the trinomial case, by plotting outcomes on an (x, y, z) Cartesian coordinates. This works reasonably well and provides a way to visualise the sample space of a Multinomial($n, \theta_1, \theta_2, \theta_3$) R \vec{V} as $(n+1) \times (n+2)$ points on a 2-simplex (triangle) on a sloping plane. For the project GUI, $\theta = (\frac{1}{3}, \frac{1}{3}, \frac{1}{3})$, i.e., in any trial, travel in the x , y or z directions is equally likely. The representations on Cartesian coordinates of the

sample space for a multinomial random vector with number of trials $n = 10$ are shown below in Figure 4 for $k = 2$ and $k = 3$. The 3-d version of the Quincunx has been termed the Septcunx, along Galton's nomenclature.

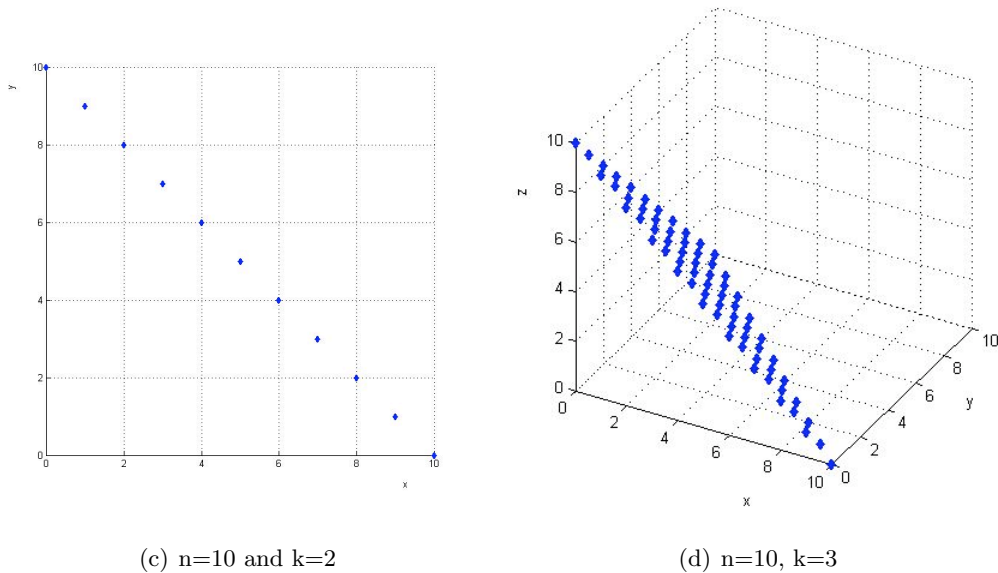


Figure 4: Binomial and trinomial sample spaces represented on Cartesian coordinates in (a) and (b), respectively.

The trinomial GUI should convey information about the probability mass function (PMF), i.e. we want to plot an outcome in the sample space in such a way that it also gives some sense of the probability of that outcome. This is achieved by scaled orthogonal projections from the plane containing the sample space. The length of the projection is proportional to the PMF for that outcome and to the number of trials n . Similarly, the proportion of realisations having a particular outcome can be represented by a version of the stem plot, or actually drawing the projected line from the representation of the outcome on the sample space plane and giving it a length proportional to the proportion of realisations having that outcome. The representations on Cartesian coordinates of the sample space with PDF-scaling for a multinomial random vector with number of trials $n = 10$ are shown below in Figure 5 for $k = 2$ and $k = 3$.

We use screen shots of our GUI in action to illustrate the results of the project. This GUI is available for download from <http://www.math.canterbury.ac.nz/lmse/quinseptcunx/>.

Figure 6 shows the Multnomial GUI in Quincunx ($k = 2$) mode, simulating first one and then 20 replications from a multinomial random vector with $n = 10$, $\theta = (\frac{1}{2}, \frac{1}{2})$. The range of the sample space is indicated with a light blue simplex (which is a 1-simplex or line for 2-dimensional coordinates (x, y)), and the area under the simplex is also filled in light blue. The outcomes in the sample space, scaled as described above, are represented with a pentagram-star and the proportion of the replications resulting in each outcome in the sample space is indicated with the stem plot. The 'history path' of a replication from the origin $(0, 0)$ to its final representation is shown below the simplex.

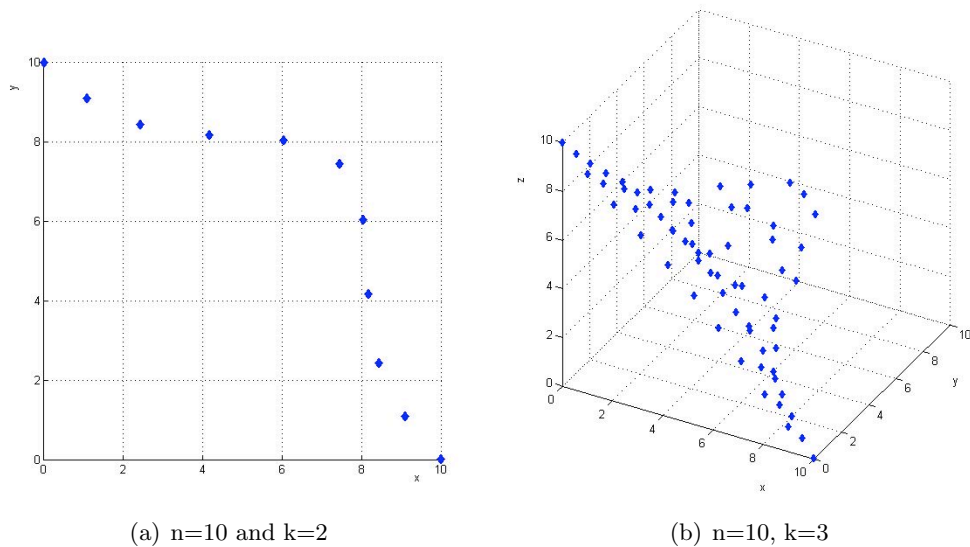


Figure 5: Binomial and trinomial PMF indicated by scaled orthogonal projection over the sample space in (a) and (b), respectively.

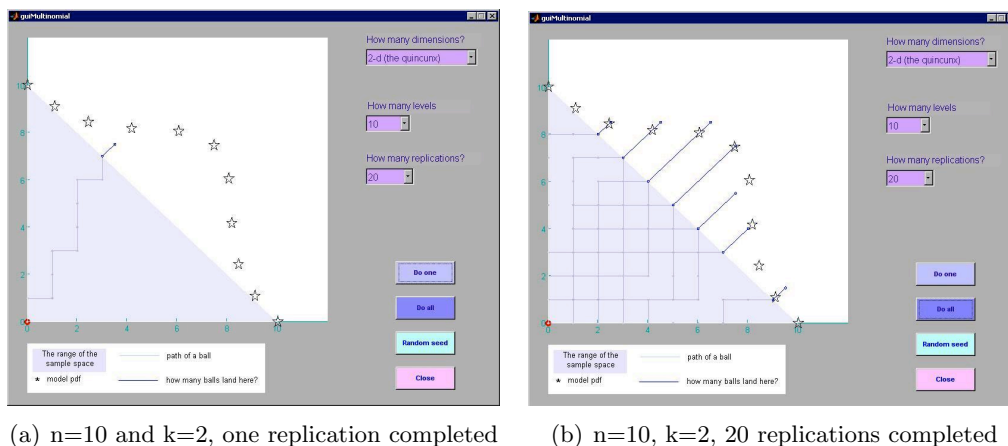


Figure 6: The Multinomial GUI in Quincunx mode

Equivalent screenshots for the Multinomial GUI in Septcunx ($k = 3$) mode are shown below in Figure 7, simulating first one and then 50 replications from a Multinomial random vector with $n = 10$, $\theta = (\frac{1}{3}, \frac{1}{3}, \frac{1}{3})$. The sample space is now the set of three dimensional non-negative integer vectors that lie on the 2-simplex or triangle whose points sum to n .

When the GUI is put into Septcunx mode a default viewing position is provided which angles the view to try to maximise the 3-d effect that the GUI aims for. The user is also provided with an additional control in the form of a slider bar which allows them to interactively rotate the Septcunx plot through about 60 degrees about the vertical axis. Figure 8 below shows the effect of rotating the view of the Septcunx using the slider.

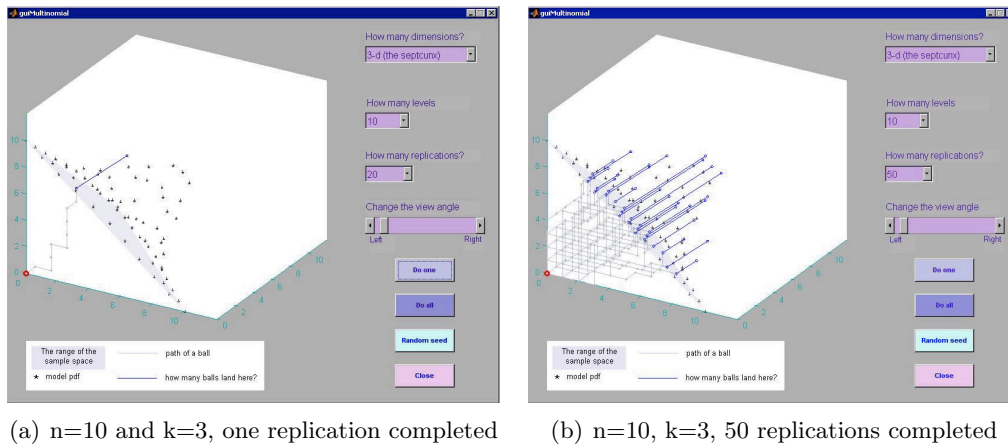


Figure 7: The Multinomial GUI in Septcunx mode

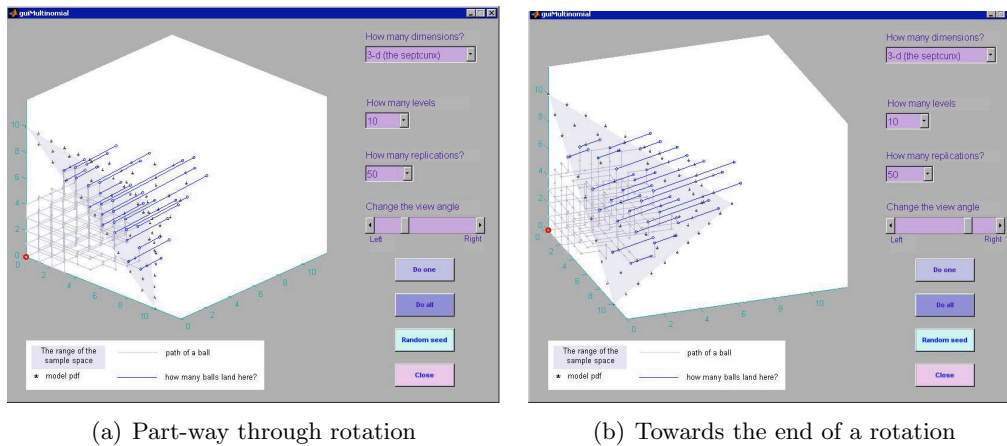


Figure 8: The Multinomial GUI in Septcunx mode with $n = 10$, $k = 3$, and 50 replications completed

4. Conclusion and Potential Modification

This project has explored how multinomial GUIs based on vector addition can be used as visual cognitive tools (VCTs) to enhance student learning of the multinomial distribution. The binomial and trinomial distributions are visually presented from their Quincunx and Septcunx constructions along with their corresponding combinatorial coefficients as the number of distinct paths to reach a given sample point. The project GUIs do this by adapting graphical displays in the following ways:

- Break processes into steps with illustrations of each stage, highlighting important points;
- Allow the user to compare the effects of using different parameters;
- Allow the user controlled interaction with the data and displays;

- Provide the graphical data displays for the user so that the user is not distracted by the mechanics of creation.

GUI design and human interaction technologies are specialised fields in their own right. This project is intended as a demonstration of the potential for GUIs as VCTs, and the actual GUIs created probably violate most if not all of the rules for good GUI design. Considerable improvements could be made on the design of these GUIs as human/technology interfaces. In addition the programming could undoubtedly be improved and made cleaner and more efficient.

The major disadvantage of the Cartesian coordinate representation is that it is not good for representing $k > 3$ Multinomial RVs. An alternative representation which retains some aspects of the travel/direction analogy but which can be adapted for higher dimensions is the use of orbit plots or tours. An orbit plot uses multiple axes and projects a high-dimensional representation into a number of low-order representations on the different axes (Young, Valero-Mora and Friendly, 2006). This would be interesting to explore but is beyond the scope of this project.

The GUI could also be expanded, or different versions created, to illustrate other related aspects. For example, with the Multinomial GUI, one could emulate Galton's original purpose of the Quincunx as well as the Septcunx, its three-dimensional extension, or illustrate basic likelihood concepts as in Ashman and Lawrence (2007), Bernoulli's Law of Large Numbers and the Central Limit Theorem. With some additional work, one can provide a visual derivation of the limiting Poisson approximation of the biased binomial distribution as well as an animated interactive derivation of Pearson's Chi-squared distribution with 1 or 2 degrees of freedom.

More ways in which the user can move and rotate the plot of multinomial outcomes could be added to the Multinomial GUI. More emphasis could be given to the meaning of the multinomial coefficient $\binom{n}{x_1, x_2, \dots, x_k} = \frac{n!}{x_1! x_2! \dots x_k!}$, possibly by tracking how many different paths in the cartesian representation of the multinomial can lead to each outcome.

5. Acknowledgements

Jennifer Harlow was supported by a studentship from the University Centre for Teaching and Learning. Bry Ashman was supported by a grant from the Department of Mathematics and Statistics. R.S. thanks Günter Steinke for a pointer to the structure of carbon atoms in diamond – the septcunx lattice. We are grateful to Anna MacDonald, Dominic Lee and Bill Taylor for their comments on earlier drafts.

6. References

Ashman, B. and Lawrence, R. (2007). Estimating the binomial probability p for Galton's Quincunx. In *Computational statistical experiments: STAT218-07S2(C) Student Projects Report UCDMS 2008/5* (pp. 47-51). Retrieved October 4, 2008, from <http://www.math.canterbury.ac.nz/~r.sainudiin/courses/STAT218/projects/Stat218StudentProjects2007>.

pdf.

Card, S.K., Mackinley, J.D. and Shneiderman, B. Eds. (1999). *Readings in information visualization: Using vision to think*. San Francisco, CA: Morgan Kaufmann.

Galton F. (1889). *Natural Inheritance*, Macmillan. Publicly available from <http://www.galton.org/books/natural-inheritance/index.html>

Nolan, D. and Temple Lang, D. (2003). *Case Studies and computing: Broadening the scope of statistical education*. Retrieved October 14, 2008, from <http://www.stat.berkeley.edu/~nolan/Papers/isi03.pdf>.

Sedig, K. and Liang, H. (2008). Learner-information interaction: A macro-level framework characterizing visual cognitive tools. *Journal of Interactive Learning Research*, 19(1), 147-173.

Tufte, E.R. (1983). *The visual display of quantitative information*. Cheshire, CN: Graphics Press.

Tukey, J.W. (1977). *Exploratory data analysis*. Reading, MA: Addison-Wesley.

Young, F., W., Valero-More, P.M. and Friendly, M. (2006). *Visual Statistics: Seeing data with dynamic interactive graphics*. Hoboken, NJ: John Wiley & Sons.